



**17th International Meeting on
Fully 3D Image Reconstruction in
Radiology and Nuclear Medicine**

Proceedings of 17th International Meeting on

**Fully 3D
Image Reconstruction
in
Radiology
and
Nuclear Medicine**

(Fully3D 2023)

Node-Based Motion Estimation Algorithm for Cardiac CT Imaging

Seongjin Yoon¹, Alexander Katsevich^{1,2}, Michael Frenkel¹, Qiulin Tang³, Liang Cai³, Jian Zhou³, and Zhou Yu³

¹iTomography Corporation, Houston, Texas 77098, USA

²Department of Mathematics, University of Central Florida, Orlando, Florida 32816, USA

³Canon Medical Research USA, Inc., Vernon Hills, Illinois 60061, USA

Abstract Proposed is a semi-iterative whole heart Motion Estimation (ME) algorithm. ME is performed in an iterative fashion in small neighborhoods of motion nodes. Location of the nodes is selected according to a new scheme. Then the nodes are ordered in a tree-like structure based on spatial proximity. The motion of each node is described by a parameterized model, and the motion model at each node is estimated almost independently of the motion of the other nodes. ME at the nodes is performed sequentially according to the selected ordering. During ME, we reconstruct local patches, which are small volumes centered at the motion nodes. Reconstruction is done using short-scan data and the current motion model. Selecting the best motion model is performed by minimizing a motion artifact metric (MAM). Our MAM is the sum of two terms. The first one measures similarity between patches reconstructed from two different short-scan ranges. The second term measures image sharpness at reference phase. Once ME for all nodes is complete, a global motion model is computed by interpolating the estimated local models. Finally, the global model is used for motion compensation in an FDK algorithm. Numerical experiments show that the algorithm is robust and provides good image quality.

1 Introduction

Despite the increased gantry rotation speed (of ~ 0.25 sec per rotation in most advanced scanners presently available), cardiac imaging still suffers from motion artifacts. A number of software-based approaches for improving temporal resolution and reducing motion artifacts have been proposed. The vast majority of such approaches are based on estimating the motion of the heart. Fully iterative algorithms, which estimate both the volume at reference time and the motion model, are usually time consuming and not suitable for clinical practice [1]. Approaches, which are based on performing motion estimation (ME) first using some shortcuts, are more efficient. A group of popular approaches is based on reconstructing subphase volumes (partial angle reconstructions, or PARs) and using them for ME [2–4]. One option is to perform ME by registering pairs of PARs that have been reconstructed at pairs of points separated by 180° (e.g., as in [2]). Another option is to warp the PARs according to some motion model and add them all up to produce the full image. The optimal motion model is selected by minimizing some motion artifact metric (MAM). The choice of a MAM is usually a difficult task. Finding the optimal motion model is a difficult task too, because the cost functional is highly non-convex and multiple local minima exist [5]. One way to overcome these difficulties is to use an artificial neural network (ANN)[6, 7]. However, the use of ANNs has its own challenges, which include getting ground

truth data, stability of the results with respect to fluctuations in HU values, and others. In this paper we develop an ME algorithm based on PARs and MAM, but we do not use an ANN. Instead, the difficulties inherent in the task are solved by using some novel ideas.

2 Algorithm description

Our cardiac Motion Estimation and Motion Compensation (ME-MC) algorithm is semi-iterative. It combines locally-iterative motion estimation (in a neighborhood of scattered motion nodes) with analytic motion compensation. The motion of each node is described by a parameterized model, and motion parameters at each node are estimated almost independently of all other nodes. The algorithm begins with the following three steps: (1) determining positions of the nodes, (2) ordering the nodes, and (3) sequential motion estimation at each node by following the selected order. Motion estimation at each node is iterative. Given the current motion model we reconstruct three versions of the same patch using three different short scan subsets of the available projection data. A patch is a small volume centered at a motion node, and the reconstructions are motion compensated. Then we evaluate the quality of the motion-compensated patches based on a cost functional. The functional measures volume similarity between the two versions of the same patch and their volume sharpness. Once motion estimation at all nodes is complete, we perform the final two steps: (4) finding a global motion model of the heart by interpolating the local motion models found in step (3), and (5) performing motion compensated reconstruction using the global motion model found in step (4).

2.1 Motion estimation

To evaluate the motion at each node independently, we use a set of patches, and compute the cost functional within each patch. For the purposes of local motion estimation, we assume that the motion does not change much within each patch, so the assumption of rigid body motion is made. Note that we assume rigid body motion only for local motion estimation. The global motion model used for the final motion compensation is elastic.

Our cost functional requires three patches reconstructed using three different short-scan data ranges, we call them SS-ref, SS-0 and SS-1. They are subsets of the total

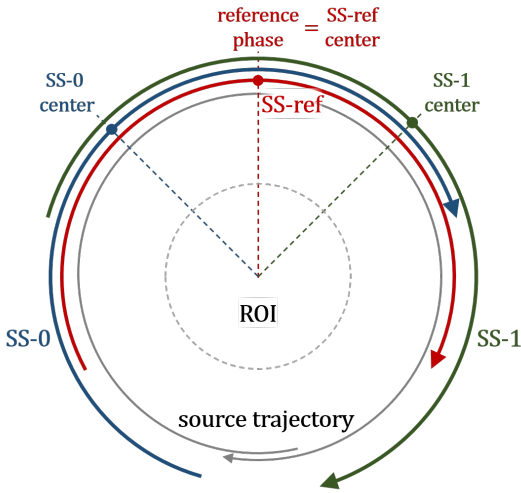


Figure 1: Schematic diagram of the short-scan ranges for SS-0, SS-1, and SS-ref, shown on the source trajectory. Solid dots are the short-scan center phases of the corresponding short-scans.

scan range, which is assumed to be slightly larger than one full rotation. SS-ref is the short-scan range, which is centered at the reference phase. This range is used for the final reconstruction. Note that our algorithm neither assumes nor requires that reference phase be the phase where the cardiac motion is minimal. The algorithm successfully reconstructed a motion-compensated volume with the maximum estimated speed reaching 78 mm/s at some nodes. SS-0 and SS-1 are short-scan ranges with their centers at equal distance from the reference phase and on opposite sides of it. Figure 1 illustrates the three short-scan ranges.

2.1.1 Cost functional and its components

For each motion node, we use the following cost functional to estimate the motion:

$$\hat{\mathbf{M}}_j = \arg \min_{\mathbf{M}} \phi_j^s(\mathbf{M}) + \gamma_j^p \phi_j^p(\mathbf{M}) + \gamma_j^{\text{reg}} \phi^{\text{reg}}(\mathbf{M}), \quad (1)$$

where

- \mathbf{M} is the set of motion parameters,
- ϕ^s is the volume similarity cost functional,
- ϕ^p is the volume sharpness cost functional,
- ϕ^{reg} is the motion parameter regularizer,
- γ is the strength parameter of the corresponding component ϕ_t ,

2.1.2 Volume similarity

Let $F_j^0(\mathbf{M})$, $F_j^1(\mathbf{M})$, and $F_j^{\text{ref}}(\mathbf{M})$ denote motion compensated, reconstructed patches centered at the j -th node using short-scans SS-0, SS-1, and SS-ref, respectively. When the motion near the node is properly estimated and compensated, the reconstructed volumes centered at

different phases should be almost identical. Therefore, we use the sum of squared differences between $F_j^0(\mathbf{M})$ and $F_j^1(\mathbf{M})$ to gauge how accurate the motion model \mathbf{M} is. We call the resulting value volume similarity ϕ^s , and it is the first part of our MAM.

$$\phi_j^s(\mathbf{M}) = \frac{1}{N_j} \|F_j^0(\mathbf{M}) - F_j^1(\mathbf{M})\|_2^2. \quad (2)$$

Here N_j is the number of voxels in the patch around the j -th node.

2.1.3 Volume sharpness

Image sharpness is used as the second part of the MAM. We estimate image sharpness by summing a vector norm of the spatial gradient over the voxels in the patch. Generally, imaging of moving objects produces blurry images. However, CT reconstruction of moving objects produces not only a blurry image, but also a depression artifact, which is characterized by image values that are too low. Frequently, these values are much lower than the average reconstructed value inside the patch. Depression artifacts tend to increase sharpness and cause bad local minima of MAM. To reject the sharpness increase due to a depression artifact, we apply a soft-thresholding function $G(\mathbf{x})$, which downweights the sharpness value around the depression artifact. Detection of depression artifacts is performed by analyzing image values. Since the final reconstruction is done for the SS-ref, we maximize the sharpness of $F_j^{\text{ref}}(\mathbf{M})$ as part of MAM to estimate motion. Let \mathbf{x} denote the vector of voxel spatial coordinates, and $f_j^{\text{ref}}(\mathbf{x}, \mathbf{M})$ denote the value of the motion compensated reconstruction F_j^{ref} at the voxel \mathbf{x} . Then, we define the volume sharpness cost functional as follows:

$$\phi_j^p(\mathbf{M}) = -\frac{1}{N_j} \sum_i \left\| \nabla f_j^{\text{ref}}(\mathbf{x}_i, \mathbf{M}) \right\|_p^p G(\mathbf{x}_i), \quad (3)$$

where p is the exponent in the L_p vector norm.

2.1.4 Regularization

Minimization of the sum of the volume similarity and sharpness cost functionals with respect to \mathbf{M} can be used to estimated motion. However, this sum is highly non-convex, there are many local minima, and it is often difficult to find the global minimum without an exhaustive search.

To use a gradient-based optimization technique, regularization is required to avoid undesirable local minima. We achieve this by penalizing various non-physical features, such as an excessively large motion amplitude and a non-smooth change in space.

To make motion estimation more stable, we also adjust the regularization strength γ_j^{reg} and the patch size for each node depending on image features inside the patch.

2.2 Node distribution

The distribution of motion nodes inside the heart is designed in such a way so that the following two conditions are satisfied: (1) motion nodes are distributed in an optimal fashion so that the minimum number of nodes can be used to accurately represent the motion of the entire heart; and (2) motion nodes are placed only in the regions where sufficiently distinctive features (e.g., strong edges) are present. This ensures the robustness of motion estimation.

To satisfy condition (2), we distribute the nodes in regions where anatomically significant features and/or significant motion is present. Motion significance is measured in an automated fashion by computing the edge difference between uncompensated reconstructions of SS-0 and SS-1. While the same overall algorithm is used to estimate motion at all nodes, some parameters of the cost functional may vary from node to node depending on anatomical characteristics of the image near the node.

2.3 Warm-start sequence

As was mentioned earlier, the motion estimation cost functional has multiple local minima, and gradient-based optimization often fails to converge to the desired minimum. Along with the regularization described in section 2.1.4, we use a predetermined warm-start sequence during motion estimation to improve robustness of the algorithm. The idea is to estimate the motion of each node one by one sequentially, so that iterative motion estimation at one node is warm-started by the motion model computed at an already processed, nearby node (called the parent node below). Creating a warm-start sequence requires sorting the nodes. Let \mathbf{N}_k , $k = 1, 2, \dots$, denote the desired node sequence. The goal of the sorting is to make sure that for each node in the sequence \mathbf{N}_k , $k \geq 2$, there is another node earlier in the sequence \mathbf{N}_m , $m < k$, so that $\text{dist}(\mathbf{N}_m, \mathbf{N}_k)$ is below a threshold. The node \mathbf{N}_{m_k} , $m_k < k$, for which this distance is minimal is called the parent node of \mathbf{N}_k . This ensures that the change of motion parameters between a node and its parent node is small. The sorting algorithm works as follows. The algorithm is initiated by creating two sets of nodes: sorted and unsorted. Initially, the list of sorted nodes contains only a starting node, which is located at the start of the RCA, and the list of unsorted nodes contains all the other nodes. Then the following steps are performed. (1) Find the closest (in terms of the Euclidean distance) node pair between the sorted nodes and unsorted nodes. (2) Remove the identified unsorted node from the unsorted node list and append it to the end of the sorted node list. The other (already sorted) node from the optimal pair is marked as the parent node for the newly added node. (3) Repeat (1) and (2) until the unsorted node list is empty.

Once node sorting is over, we run motion estimation at each node as described in section 2.1 by following the order in

the sorted node list. Motion estimation at the first node starts with the zero motion. Motion estimation at each subsequent node is warm-started using the estimated motion at its parent node.

3 Test results

We present reconstruction results for clinical datasets acquired using a Canon Aquilion ONE 320-slice CT scanner. A total of 22 clinical datasets were tested, and all results showed good improvement after ME-MC is applied. Figures 2 to 5 show four clinical data examples of our ME-MC FDK reconstructions compared with the uncorrected FDK reconstructions. The uncorrected images are on the left, and the corresponding corrected ones - on the right. Comparing the locations marked by arrows, we see that the algorithm provides good image quality.

4 Conclusions

In this work, we presented a computationally inexpensive algorithm for cardiac motion estimation and motion compensation. The algorithm is based on MAM minimization, and a number of ideas have been implemented in order to avoid false local minima. Numerical experiments show that the algorithm is robust and provides good image quality.

5 Acknowledgements

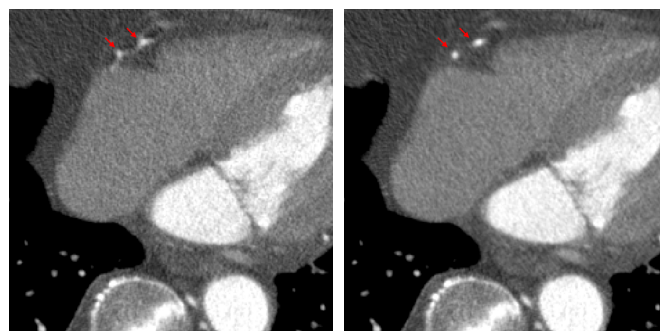
Clinical images courtesy of Dr. Marcus Chen, National Heart, Lung and Blood Institute, National Institutes of Health, USA.

A. Katsevich is a shareholder and chief technology officer of iTomography Corporation and, as such, may benefit financially as a result of the outcomes of the work reported in this publication.

References

- [1] Q. Tang, J. Cammin, S. Srivastava, et al. "A fully four-dimensional, iterative motion estimation and compensation method for cardiac CT". *Medical Physics* 39 (2012), pp. 4291–4305.
- [2] S. Kim, Y. Chang, and J. B. Ra. "Cardiac motion correction based on partial angle reconstructed images in X-ray CT". *Medical Physics* 42 (2015), pp. 2560–2571.
- [3] S. Kim, Y. Chang, and J. B. Ra. "Cardiac Image Reconstruction via Nonlinear Motion Correction Based on Partial Angle Reconstructed Images". *IEEE Transactions on Medical Imaging* 36.5 (2017), pp. 1151–1161. DOI: [10.1109/TMI.2017.2654508](https://doi.org/10.1109/TMI.2017.2654508).
- [4] J. D. Pack, A. Manohar, S. Ramani, et al. "Four-dimensional computed tomography of the left ventricle, Part I: Motion artifact reduction". *Medical Physics* July 2021 (2022), pp. 4404–4418. DOI: [10.1002/mp.15709](https://doi.org/10.1002/mp.15709).

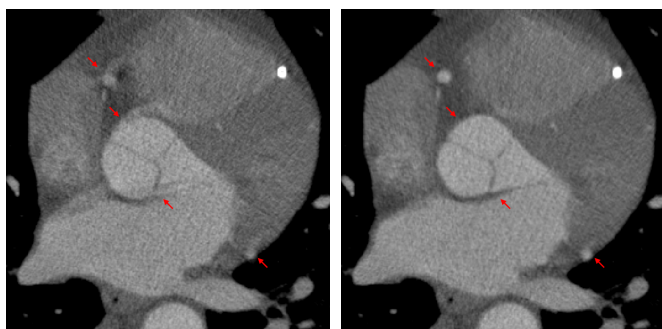
- [5] J. Hahn, H. Bruder, C. Rohkohl, et al. "Motion compensation in the region of the coronary arteries based on partial angle reconstructions from short-scan CT data". *Medical Physics* 44.11 (2017), pp. 5795–5813. DOI: [10.1002/mp.12514](https://doi.org/10.1002/mp.12514).
- [6] G. Quan, J. Tian, and Y. Wang. "Cardiac Motion Correction of Computed Tomography (CT) with Spatial Transformer Network". *Proceedings of the 6th International Conference on Image Formation in X-Ray Computed Tomography* (2020), pp. 82–85.
- [7] J. Maier, S. Lebedev, J. Erath, et al. "Deep learning-based coronary artery motion estimation and compensation for short-scan cardiac CT". *Medical Physics* 48.7 (2021), pp. 3559–3571. DOI: [10.1002/mp.14927](https://doi.org/10.1002/mp.14927).



(a) Uncorrected FDK

(b) ME-MC FDK

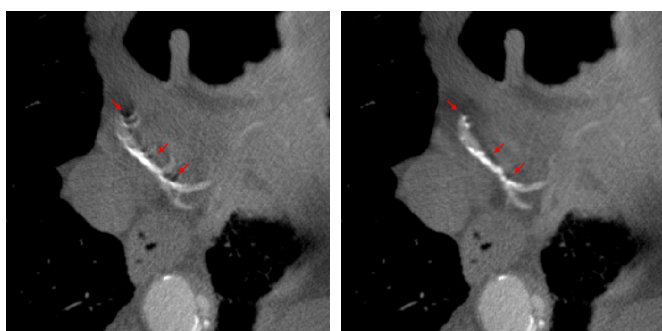
Figure 5: Example of ME-MC results, fourth dataset. Maximum estimated motion speed is 45 mm/s.



(a) Uncorrected FDK

(b) ME-MC FDK

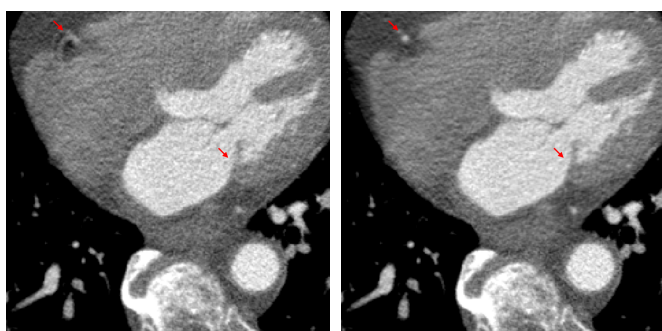
Figure 2: Example of ME-MC results, first dataset. Maximum estimated motion speed is 78 mm/s.



(a) Uncorrected FDK

(b) ME-MC FDK

Figure 3: Example of ME-MC results, second dataset. Maximum estimated motion speed is 46 mm/s.



(a) Uncorrected FDK

(b) ME-MC FDK

Figure 4: Example of ME-MC results, third dataset. Maximum estimated motion speed is 63 mm/s.